Variability of rill detachment capacity with sediment size, water depth and soil slope in forest soils: A flume experiment

Variability of rill detachment capacity with sediment size, water depth and soil slope in forest soils: a flume experiment

Misagh Parhizkar [1,] Mahmood Shabanpour [1], Manuel Esteban Lucas-Borja [2], Demetrio Antonio Zema [3]*

[1] Department of Soil Science, Faculty of Agricultural Sciences, University of Guilan, Rasht, Iran

[2] Escuela Técnica Superior Ingenieros Agrónomos y Montes, Universidad de Castilla-La Mancha. Campus Universitario, E-02071, Albacete, Spain

[3] Department AGRARIA, Mediterranean University of Reggio Calabria, Loc. Feo di Vito, I-89122, Reggio Calabria, Italy

* Correspondence: misagh.parhizkar@gmail.com

Abstract

Rill detachment is the most important erosive process in steep slopes and its comprehension and prediction accuracy is important to properly develop soil conservation practices in forest areas. This process is largely influenced by sediment size, soil slope and water flow characteristics, but the results of the studies that have explored these influences are contrasting. This study has simulated in an experimental flume the rill detachment capacity (D_c) of soil with five particle sizes (0-0.25, 0.25-0.5, 0.5-1, 1-2, and 2-3 mm) at five water flow rates (0.26, 0.35, 0.45, 0.56, and 0.67 L m^{-1} s^{-1}) and five bed slopes (3.5%, 9.1%, 19.2%, 29.1%, and 38.3%) on samples collected in a forestland of Northern Iran. D_c was significantly higher (by 70%) for sediments size over 1 mm compared to the other soil fractions and increased primarily with soil slope and secondarily with water depth. A modelling approach has shown that the unit stream power is the best predictor of D_c using power equations (NSE over 0.87). Linear regression models between D_c and shear stress (τ) were very accurate (r^2 over 0.80 with few exceptions) in predicting both rill erodibility and critical shear stress, when developed separately for each particle size class. Sediments with size higher than 1 mm had lower resistance to rill erosion compared to the finer fractions. Overall, the study helps to better understand particle detachment of the erosion process, on which particle size is a key parameter. The modelling activity proposes to land planners

values of the rill erodibility and critical shear stress of forested areas for applications in process-based erosion models.

Keywords: Shear stress; Rill erodibility; Plantation; Unit stream power; Rill erosion; Different sizes of sediment.

1. Introduction

Soil erosion is a severe threat for ecosystem health in many parts of the world (Rodrigo-Comino et al., 2018; Cerdà et al., 2021; Borrelli et al., 2021; Bezak et al., 2021). In the water erosion process, overland flow is the most important agent of particle detachment together with raindrop impact. Erosion in rills is dominant compared to laminar erosion in steep hillslopes. Moreover, rill erosion is different between shallow or deep waters as well high low and high flow rates (Zhang et al., 2002).

Soil detachment by shallow flow happens when the maximum force exerted by highly turbulent water is greater than the resistance between soil particles. Sediment size plays an important role in the soil detachment process, since the particle dimensions influence the turbulence and detachability in sediment-laden flow (Liu et al., 2019). However, the influence of sediment size in reducing or increasing soil detachment rates is sometimes contrasting in literature, due to the different experimental conditions and the number of factors influencing particle detachment (e.g., soil slope, water flow rates, sediment concentration). For example, Ali et al. (2012) and Liu et al. (2019) state that rill detachment is different from finer to coarser sediments. The experimental results by Ali et al. (2012) showed that the flow velocity (and therefore soil detachment) decreases with increasing median grain size. According to Liu et al. (2019), the sediment median size had a pronounced negative impact on the detachment rates. Similarly, Nearing et al. (1991) found that the detachment rate of soils with coarse particles increases compared to finer soils. Conversely, Merten et al. (2001) showed that detachment rate increases with decreasing sediment size. Thus, more research is needed, in order to clarify these waiving results of the literature studies. Rill detachment capacity may be even different in soils that, although being of the same type and use, and subjected to the same management, are covered by different tree species (Parhizkar et al., 2021a). The root system of plants may influence soil aggregate stability and therefore soil detachment (De Baets et al., 2006). Moreover, the rill detachment rates in reforested soils are significantly higher compared to the values

measured in natural forests (Parhizkar et al., 2021b). Therefore, it is important to investigate the importance of sediment size on soil detachment in reforested soils. When soil is planted with trees, an accurate evaluation of the areas that are more exposed to rill erosion is essential, in order to choose the most protective species (Pollen, 2007; Vanoppen et al., 2015; 2017). Thus, the estimation of soil detachment capacity together with the factors that influence this parameter is important to assess not only whether a soil is exposed to non-tolerable erosion rates.

Erosion models are useful tools to help land managers adopting the most effective anti-erosive practices (Parhizkar et al., 2021d). Many process-based erosion models use soil detachment capacity as key input parameter (Nearing et al., 1989, 1999; Li et al., 2015). Therefore, accurate estimations of rill detachment capacity are essential to achieve reliable predictions in forest ecosystems that are prone to erosion. This study has analysed the rill detachment capacity through flume experiments on soils sampled in a reforested area with steep slopes of Northern Iran. More specifically, we have (i) evaluated the impact of different sediment size on soil detachment rate at variable water flow rates and soil slopes, and (ii) setup simple models to predict the soil detachment capacity and rill erodibility from hydraulic parameters for each studied sediment size. We hypothesize that the rill detachment process is significantly variable with sediment size with higher detachability of coarser soil fractions and steeper soils, and the prediction models developed in this study are able to take into account this variability.

2. Materials and methods

2.1. Study area

The experiments were conducted in the laboratory of soil physics at the Guilan University (Iran) on soil samples collected in the Saqalaksar Forestland Park (37°09’24”N, 49°31’50”E, Northern Iran) (Figure 1). The park is located in Guilan province, 15 km south of Rasht city, at an elevation of about 60 m above the mean sea level. The climate conditions of the area are typically Mediterranean, Csa type (Koppen–Geiger classification, Kottek et al., 2006), with mean annual values of precipitation and temperature of 1360 mm and 16.3 ◦C, respectively (IRIMO, 2016).

The soil of the park is silty clay loamy (according to the USDA classification), on average 33.5% of clay, 46.8% of silt and 19.6% of sand. The mean organic matter content of soil

1.42%. Moreover, the mean soil bulk density of soil is 1.2 g/cm^3 (Parhizkar et al., 2021c). Other soil properties are reported in Parhizkar et al. (2021a).

The vegetal biodiversity in the park is large, with a great variety of tree and shrub species, mainly *Zelkova carpinifolia*, *Quercus castaneifolia*, *Alnus glutinosa*, *Parrotia persica*, *Pinus taeda*, and *Carpinus betulus* (80% of the park area). Beside these natural species, other species were planted in this forestland and then subjected to different management operations, such as harvesting, tree planting and fires (Parhizkar et al., 2021c). Some of these management practices, targeted to rehabilitation of this forestland, have modified soil properties, including soil detachment capacity (Parhizkar et al., 2021a).

2.2. Soil sampling

Soil was randomly but uniformly sampled in different points of the experimental area, about one samples each 2000 m^2 (Figure 1). After sampling, soil was transferred to the laboratory, where each sample was separated into five sediment size classes: (i) 0-0.25 mm (clay, silt, and very fine to fine sand); (ii) 0.25-0.5 mm (medium sand); (iii) 0.5-1 mm (coarse sand); (iv) 1-2 mm (very coarse sand); and (v) 2-3 mm (gravel). Sieves with meshes of 4, 2, 1 and less than 1 mm were used, respectively. Hereinafter, the five classes will be indicated using the mean value of the range: (i) 0.125 mm for clay, silt, and very fine to fine sand; (ii) 0.375 mm for medium sand; (iii) 0.75 mm for coarse sand; (iv) 1.5 mm for very coarse sand; and (v) 2.5 mm for gravel.

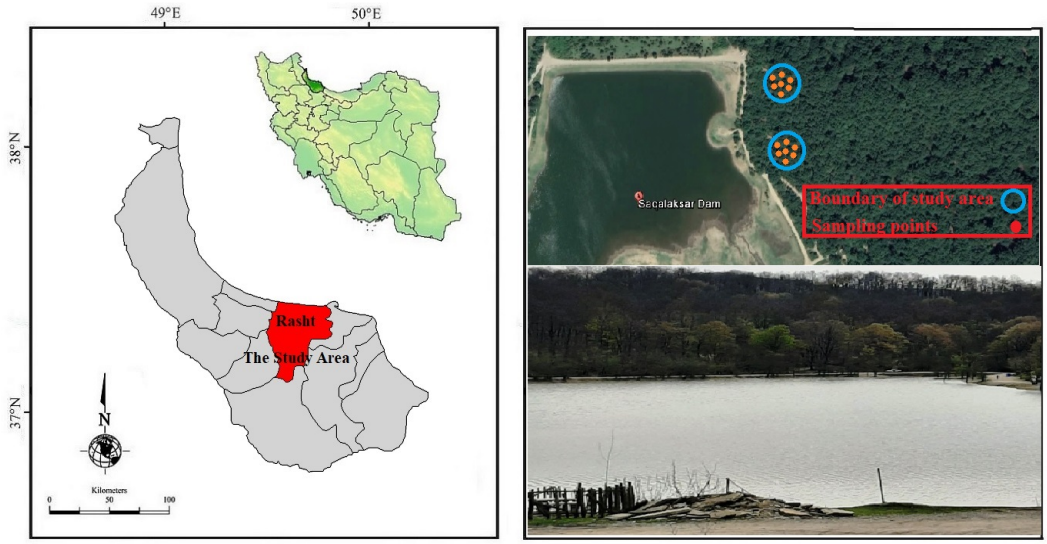

Figure 1 - Aerial map (left), Geographical location and the sampling point (right) of the study area (Saqalaksar Forestland Park, Northern Iran). Aerial view source: Google® Maps®.

2.3. Measurement of rill detachment capacity

Rill detachment capacity (D_c, kg s^{-1} m^{-2}) of the soil samples was measured in a hydraulic flume with rectangular cross section (0.2 m x 0.2 m) and length of 3.5 m (Figure 2). More details about this flume and the experimental procedure for running the experiments are reported in Parhizkar et al. (2020a; 2020b; 2021a; 2021b).

Figure 2 - Flume installed at the Guilan University (Iran) and used for the experiments on rill detachment capacity on soils sampled in the Saqalaksar Forestland Park (Northern Iran).

The experiments were carried out for each sediment size class, and D_c was measured at five water flow rates (0.26, 0.35, 0.45, 0.56, and 0.67 L m^{-1} s^{-1}) and five gradients of the flume bed (3.5%, 9.1%, 19.2%, 29.1%, and 38.3%). Each experiment consisted of four replicates. Overall, 500 soil samples (5 sediment size classes × 5 water flow rates × 5 slope gradients × 4 repetitions) were tested.

The experimental procedure consisted of the following steps. Each soil sample was packed in a steel ring (diameter of 0.1 m and height of 0.05 m) and then was saturated by wetting for 24 h before the flume experiment. Then, the sample was inserted in a hole of the flume bed, close to the downstream outlet. After the setup of flow rate and bed gradient in the flume, the experiment started pouring water from the upstream side and a stable water level was waited for. The maximum duration of each experiment was 300 seconds, but sometime the experimental test was ended before this limit, when a depth of 0.015 m of soil was

eroded from the steel ring. After the experiment, the wet soil sample was oven-dried and weighed.

The mean flow rate was checked by collecting and measuring five samples of water downstream of the flume by a graduated plastic cylinder. Following Abrahams et al. (1985), the average water velocity was also determined as the mean of seven measurements, and this value was reduced by 0.6, 0.7, or 0.8 factors, for laminar, transitional, or turbulent conditions, respectively. The mean water depth was measured by averaging six measures in two cross sections of the flume using a level probe with accuracy of 1 mm (Parhizkar et al., 2020a). Given the importance of water depth for the evaluation of D_c, the accuracy of this measure was further checked using a self-made digital instrument. In summary, this device consisted of two sections, of which the first was a printed circuit board (PCB) for the detection of the water level in the flume, and the second contained a junction box and a LED display.

D_c was calculated as the mean value of the four replicates of each experiment at a given flow rate and bed gradient using equation (1).

$$D_c = \frac{\Delta M}{A \cdot \Delta t} \quad (1)$$

In this equation, ΔM is the dry weight of detached soil sample (in kg), Δt is the test duration (in s) and A is the area of the soil sample (in m^2).

In addition to the flow rate (Q, L m^{-1} s^{-1}), depth (m) and velocity (m s^{-1}), the other hydraulic parameters measured in each experiment were the shear stress (τ, Pa), stream power (Ω, kg s^{-3}), unit stream power (ω, m s^{-1}) and unit flow energy (E, m). The equations to calculate these parameters are reported in Parhizkar et al., 2020a and 2020c, while the related values measured or calculated for each experiment are reported in Table 1.

The rill erodibility (K_r) and critical shear stress (τ_c), which are important parameters for estimating soil resistance to rill erosion (Wang et al., 2014), were calculated as the slope and intercept of the following equation regressing D_c and τ:

$$D_C = K_r(\tau - \tau_c) \quad (2)$$

Table 1 - Hydraulic parameters measured or calculated in experiments for measuring the rill detachment capacity in the Saqalaksar Forestland (Northern Iran).

Experiment ID	S [m m^{-1}]	Q [L m^{-1} s^{-1}]	h [m]	V [m s^{-1}]	τ [Pa]	Ω [kg s^{-3}]	ω [m s^{-1}]	E [m]
1	0.035	0.26	0.005	0.17	1.70	0.29	0.006	0.007
2		0.35	0.006	0.24	1.91	0.46	0.008	0.009
3		0.46	0.007	0.36	2.15	0.78	0.013	0.013
4		0.57	0.008	0.45	2.60	1.17	0.016	0.019
5		0.69	0.009	0.56	2.89	1.62	0.020	0.025
6	0.091	0.26	0.004	0.27	3.59	0.97	0.025	0.008
7		0.35	0.005	0.38	4.49	1.71	0.035	0.013
8		0.45	0.006	0.52	5.21	2.71	0.047	0.020
9		0.56	0.007	0.61	6.07	3.70	0.056	0.026
10		0.67	0.008	0.68	6.91	4.70	0.062	0.032
11	0.192	0.26	0.003	0.33	4.77	1.57	0.063	0.008
12		0.35	0.004	0.43	6.36	2.74	0.083	0.013
13		0.45	0.005	0.55	9.47	5.21	0.106	0.021
14		0.56	0.006	0.66	11.32	7.47	0.127	0.029
15		0.67	0.007	0.74	12.96	9.59	0.142	0.035
16	0.291	0.26	0.002	0.37	5.04	1.87	0.108	0.009
17		0.35	0.003	0.47	8.57	4.03	0.137	0.014
18		0.45	0.004	0.57	11.76	6.70	0.166	0.021
19		0.56	0.005	0.71	14.61	10.37	0.207	0.031
20		0.67	0.006	0.81	17.15	13.89	0.236	0.040
21	0.383	0.26	0.001	0.39	5.18	2.02	0.149	0.009
22		0.35	0.002	0.52	8.80	4.57	0.199	0.016
23		0.45	0.003	0.61	12.34	7.53	0.234	0.022
24		0.56	0.004	0.78	15.47	12.07	0.299	0.035
25		0.67	0.005	0.89	18.89	16.81	0.341	0.045

Notes: S = bed gradient; Q = flow rate; h = water depth; V = mean flow velocity; τ = shear stress; Ω = stream power; ω = unit stream power; E = unit flow energy.

211 *2.4. Statistical analysis*

212

213 Prior to the experiments, we run a 2-way ANalysis Of VAriance (ANOVA) considering the
214 rill detachment capacity as dependent variable and soil slope and flow discharge as factors
215 (independent variables, including their interaction). This allowed identifying that both soil
216 slope and flow discharge, but not their interaction, play a significant influence on D_c. Then,
217 ANOVA was applied to D_c (dependent variable) and five sediment size classes (factors). In
218 both cases, the normality of sample distribution was checked by QQ-plot tests. The
219 pairwise comparison by Tukey's test (at $p < 0.05$) was used to assess the statistical
220 significance of the differences in D_c among the various sizes of sediments.
221 Moreover, non-linear models were used to evaluate possible regressions between D_c and
222 hydraulic parameters. The models are based on power equations, as suggested in the
223 previous studies (Parhizkar et al., 2020a; 2020c; 2021a). The Root Mean Square Error
224 (RMSE), Nash-Sutcliffe Efficiency (NSE, Nash and Sutcliffe, 1970) and the coefficient of
225 determination (r^2) were used as evaluation criteria to verify the accuracy of these equations.
226 The satisfactory values of these evaluation criteria are less than 50% of observed standard
227 deviation for RMSE, over 0.35 for NSE, and over 0.50 for r^2. If NSE is over 0.75, the
228 model prediction capacity of a variable is good (Moriasi et al., 2003; Singh et al., 2008;
229 Van Liew and Garbrecht, 2003).
230 All statistical analyses were carried out using XLSTAT 9.0 software.

231

232 **3. Results**

233

234 *3.1. Variability of rill detachment capacity with sediment size, water depth and soil slope*

235

236 The preliminary ANOVA showed that both soil slope and flow rate, but not their
237 interaction ($p = 0.924$), have a significant influence ($p < 0.0001$) on the rill detachment
238 capacity (Table 2). D_c was similar ($p < 0.05$) among three sediment size classes (0.125,
239 0.375, and 0.75). In contrast, D_c of the two coarser sediment classes (1.5 and 2.5 mm) was
240 significantly ($p < 0.05$) different from the finer classes. The highest D_c was measured for
241 the coarser class (0.047 kg m^{-2} s^{-1}), while the finer sediments showed the lowest value
242 (0.0263 kg m^{-2} s^{-1}). Moreover, D_c of each class was highly variable around the mean value
243 of each class, as shown by the large standard deviations (Figure 3).

244

Table 2 - Two-way ANOVA of the rill detachment capacity on soil samples collected in the Saqalaksar Forestland (Northern Iran).

Factors	Degree of freedom	Sum of squares	Mean squares	F-value	P-value
Soil slope	4	0.100	0.025	162.095	**< 0.0001**
Flow rate	4	0.003	0.001	5.548	**0.000**
Soil slope x flow rate	16	0.001	0.000	0.533	0.924

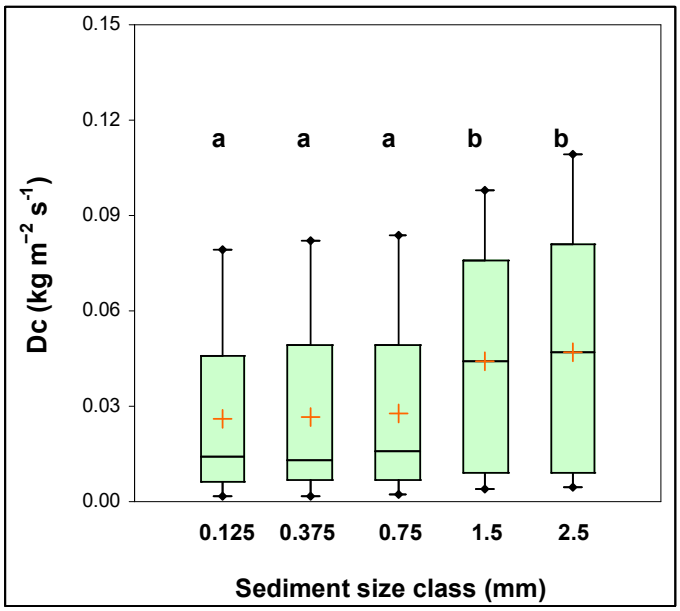

Figure 3 - Box plot of variability of rill detachment capacity (D_c) among sediment size classes of forest soils sampled in Saqalaksar Forestland Park (Northern Iran) (Different letters indicate significant differences after ANOVA at $p < 0.05$).

3.2. Relationships between rill detachment capacity and hydraulic parameters

The power equations between D_c and flow depth (h) at different soil slopes (S) and sediment size classesd showed high to very high correlations ($r^2 > 0.66$ with a maximum of 0.99) between these two variables, with D_c increasing with S and h. In each sediment class, the exponent of the equations increases with S, athough not monotonically (Table 3 and Figure 4).

264

265

266 Table 3 - Power equations correlating the rill detachment capacity (D_c, kg m^{-2} s^{-1}) with the
267 water depth (h, m) and coefficients of determination (r^2) for different sediment size classes
268 of the soil sampled in Saqalaksar Forestland Park (Northern Iran).

269

Sediment size class (mm)	**Soil slope (%)**	**Equation**	**r^2**
0.125	3.5	$D_c = 0.646\ h^{1.184}$	0.99
	9.1	$D_c = 0.347\ h^{0.772}$	0.94
	19.2	$D_c = 1.542\ h^{0.882}$	0.93
	29.1	$D_c = 0.551\ h^{0.471}$	0.99
	38.3	$D_c = 0.221\ h^{0.208}$	0.86
0.375	3.5	$D_c = 0.497\ h^{1.057}$	0.95
	9.1	$D_c = 0.334\ h^{0.761}$	0.94
	19.2	$D_c = 1.618\ h^{0.892}$	0.89
	29.1	$D_c = 0.733\ h^{0.518}$	0.97
	38.3	$D_c = 0.226\ h^{0.211}$	0.73
0.75	3.5	$D_c = 0.215\ h^{0.668}$	0.94
	9.1	$D_c = 0.259\ h^{0.916}$	0.95
	19.2	$D_c = 3.328\ h^{1.008}$	0.93
	29.1	$D_c = 0.422\ h^{0.409}$	0.99
	38.3	$D_c = 0.214\ h^{0.196}$	0.72
1.5	3.5	$D_c = 0.178\ h^{0.721}$	0.95
	9.1	$D_c = 4.468\ h^{1.185}$	0.66
	19.2	$D_c = 1.077\ h^{0.606}$	0.97
	29.1	$D_c = 0.454\ h^{0.343}$	0.94
	38.3	$D_c = 0.231\ h^{0.147}$	0.96
2.5	3.5	$D_c = 0.127\ h^{0.639}$	0.93
	9.1	$D_c = 26.238\ h^{1.507}$	0.80
	19.2	$D_c = 0.858\ h^{0.550}$	0.99

	29.1	$D_c = 0.452\ h^{0.333}$	0.95
	38.3	$D_c = 0.231\ h^{0.147}$	0.96

270

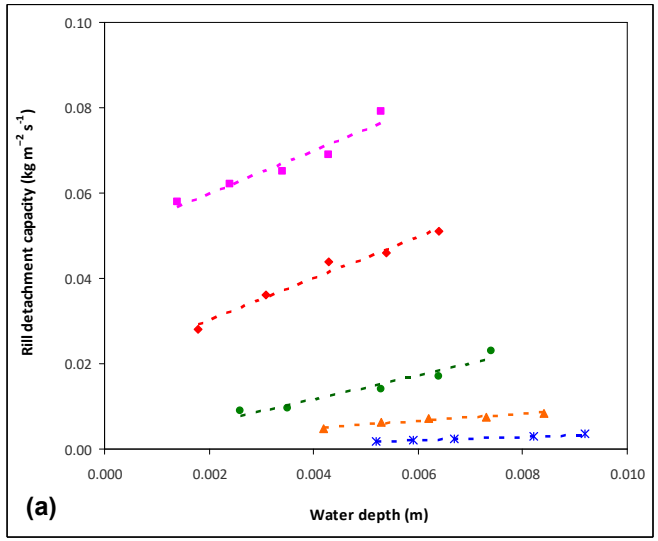

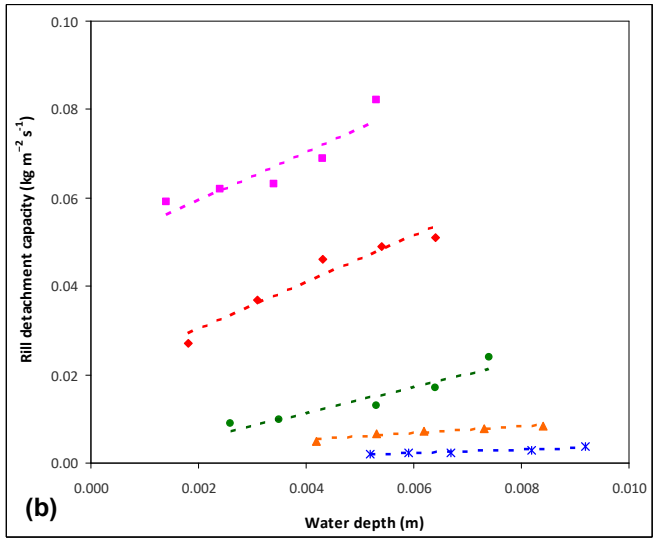

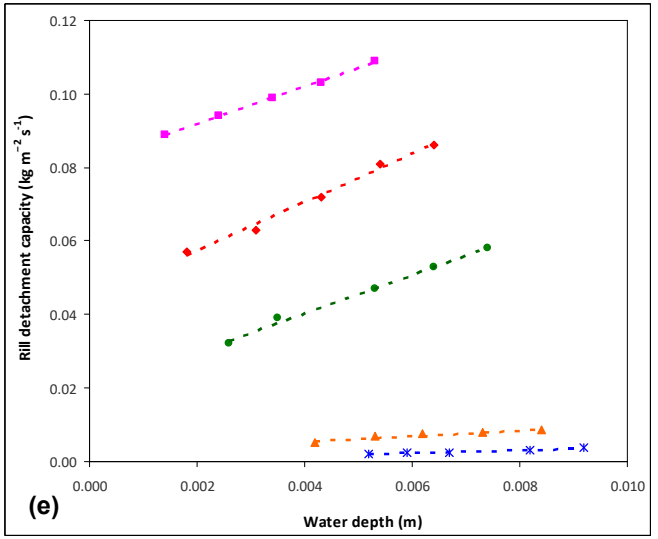

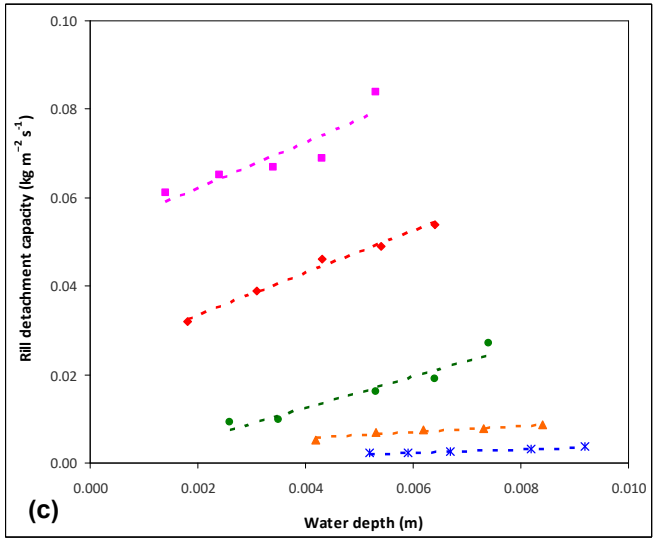

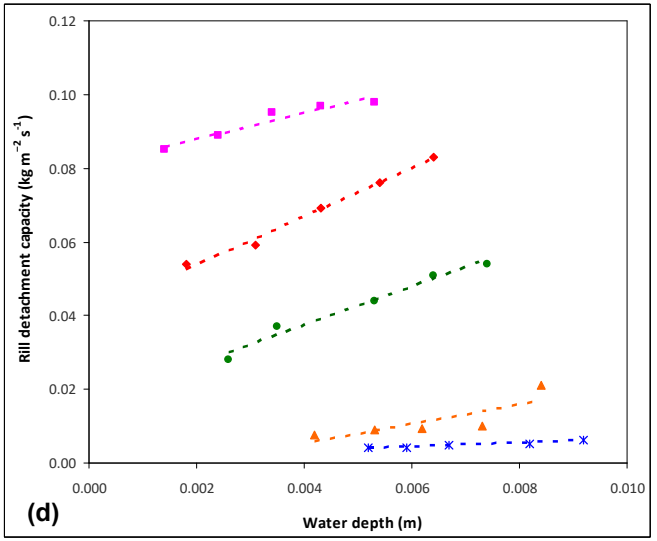

Sediment size class of soil

(a) 0.125 mm
(b) 0.375 mm
(c) 0.75 mm
(d) 1.5 mm
(e) 2.5 mm

Soil slope (%)

3.5
9.1
19.2
29.1
38.3

271

272 Figure 4 - Linear regressions between the rill detachment capacity and water depth for different soil slopes and sediment size classes of the soil
273 sampled in Saqalaksar Forestland Park (Northern Iran).

For all sediment classes, D_c was predicted with very high accuracy by power equations (1) based on the unit stream power (ω). This good prediction capacity is confirmed by the very high evaluation criteria, which were all very high (Table 4). Conversely, the equations using the stream power (Ω) and shear stress (τ) as input showed a lower, but satisfactory, prediction capacity of D_c. The mean flow velocity (V) and unit flow energy were poor predictors of D_c (Table 4).

Table 4 - Power equations predicting the rill detachment capacity (D_c, kg m^{-2} s^{-1}) from hydraulic parameters and evaluation criteria for different sediment size classes of the soil sampled in Saqalaksar Forestland Park (Northern Iran).

Variable	**Sediment size class (mm)**	**Equation**	**r^2**	**NSE**	**RMSE**
V	0.125	$D_c = 0.061\ V^{2.007}$	0.37	0.26	0.02
	0.375	$D_c = 0.061\ V^{1.991}$	0.38	0.26	0.02
	0.75	$D_c = 0.063\ V^{1.961}$	0.37	0.26	0.02
	1.5	$D_c = 0.099\ V^{1.835}$	0.38	0.27	0.03
	2.5	$D_c = 0.109\ V^{1.841}$	0.40	0.31	0.03
τ	0.125	$D_c = 0.0008\ \tau^{1.535}$	0.60	0.58	0.02
	0.375	$D_c = 0.0009\ \tau^{1.523}$	0.61	0.60	0.02
	0.75	$D_c = 0.0009\ \tau^{1.519}$	0.61	0.59	0.02
	1.5	$D_c = 0.002\ \tau^{1.461}$	0.65	0.50	0.02
	2.5	$D_c = 0.002\ \tau^{1.451}$	0.66	0.59	0.02
Ω	0.125	$D_c = 0.005\ \Omega^{0.955}$	0.55	0.53	0.02
	0.375	$D_c = 0.005\ \Omega^{0.948}$	0.56	0.53	0.02
	0.75	$D_c = 0.005\ \Omega^{0.942}$	0.56	0.51	0.02
	1.5	$D_c = 0.009\ \Omega^{0.899}$	0.58	0.52	0.02
	2.5	$D_c = 0.010\ \Omega^{0.895}$	0.60	0.55	0.02
ω	0.125	$D_c = 0.220\ \omega^{1.035}$	0.91	0.87	0.01
	0.375	$D_c = 0.218\ \omega^{1.025}$	0.91	0.87	0.01

	0.75	$D_c = 0.229\ \omega^{1.023}$	0.91	0.87	0.01
	1.5	$D_c = 0.354\ \omega^{0.980}$	0.91	0.91	0.01
	2.5	$D_c = 0.374\ \omega^{0.971}$	0.92	0.92	0.01
E	0.125	$D_c = 0.826\ E^{1.008}$	0.22	0.05	0.02
	0.375	$D_c = 0.837\ E^{1.006}$	0.11	-0.01	0.02
	0.75	$D_c = 0.805\ E^{0.984}$	0.22	0.05	0.02
	1.5	$D_c = 0.963\ E^{0.892}$	0.22	0.05	0.03
	2.5	$D_c = 1.092\ E^{0.903}$	0.23	0.07	0.04

Notes: V = mean flow velocity (m s^{-1}); τ = shear stress (Pa); Ω = stream power (kg s^{-3}); ω = unit stream power (m s^{-1}); E = unit flow energy (m); r^2 = coefficient of determination; NSE = coefficient of Nash and Sutcliffe; RMSE = Root Mean Square Error.

Grouping all the studied sediment size classes of soil, equation (2), applied to couples of D_c vs. shear stress (τ), showed good, although not very high coefficients of determination ($0.61 \leq r^2 \leq 0.70$) (data not shown). When D_c was regressed against τ separately for each sediment class, the coefficients of determination increased up to values over 0.80 (with two exceptions, soil slopes of 9.1% and sediment classes of 1.5 mm) (Table 5 and Figure 5).

Rill erodibility (K_r) and critical shear stress (τ_c) were clearly different for sediments of variable class and soil slopes. K_r generally increased with the mean diameter of the sediments, although this increase was not always uniform (Figure 6). In addition, τ_c increased with sediment diameter and soil slope (also in this case not uniformly) (Figure 7).

Table 5 – Regression equations between the rill detachment capacity (D_c, kg m^{-2} s^{-1}) and shear stress (τ), and coefficients of determination (r^2) at different soil slopes and for different sediment size classes of the soil sampled in Saqalaksar Forestland Park (Northern Iran).

Soil slope (%)	**Sediment size class (mm)**	**Equation**	***r*²**
3.5	0.125	$D_c = 0.0014\ \tau - 0.0005$	0.99
	0.375	$D_c = 0.0014\ \tau - 0.0004$	0.94

	0.75	$D_c = 0.0013\ \tau - 0.0001$	0.96
	1.5	$D_c = 0.0018\ \tau + 0.0010$	0.95
	2.5	$D_c = 0.0017\ \tau + 0.0016$	0.93
9.1	0.125	$D_c = 0.0010\ \tau + 0.0015$	0.94
	0.375	$D_c = 0.0010\ \tau + 0.0016$	0.94
	0.75	$D_c = 0.0009\ \tau + 0.0023$	0.94
	1.5	$D_c = 0.0034\ \tau - 0.0064$	0.65
	2.5	$D_c = 0.0047\ \tau - 0.0116$	0.78
19.2	0.125	$D_c = 0.0016\ \tau - 0.0003$	0.93
	0.375	$D_c = 0.0017\ \tau - 0.0009$	0.88
	0.75	$D_c = 0.0021\ \tau - 0.0023$	0.93
	1.5	$D_c = 0.0031\ \tau + 0.0152$	0.98
	2.5	$D_c = 0.0031\ \tau + 0.0182$	0.99
29.1	0.125	$D_c = 0.0019\ \tau + 0.0197$	0.97
	0.375	$D_c = 0.0020\ \tau + 0.0190$	0.94
	0.75	$D_c = 0.0018\ \tau + 0.0235$	0.99
	1.5	$D_c = 0.0025\ \tau + 0.0400$	0.99
	2.5	$D_c = 0.0025\ \tau + 0.0432$	0.99
38.3	0.125	$D_c = 0.0014\ \tau + 0.0492$	0.93
	0.375	$D_c = 0.0015\ \tau + 0.0483$	0.83
	0.75	$D_c = 0.0015\ \tau + 0.0515$	0.80
	1.5	$D_c = 0.0010\ \tau + 0.0806$	0.93
	2.5	$D_c = 0.0014\ \tau + 0.0814$	0.99

308

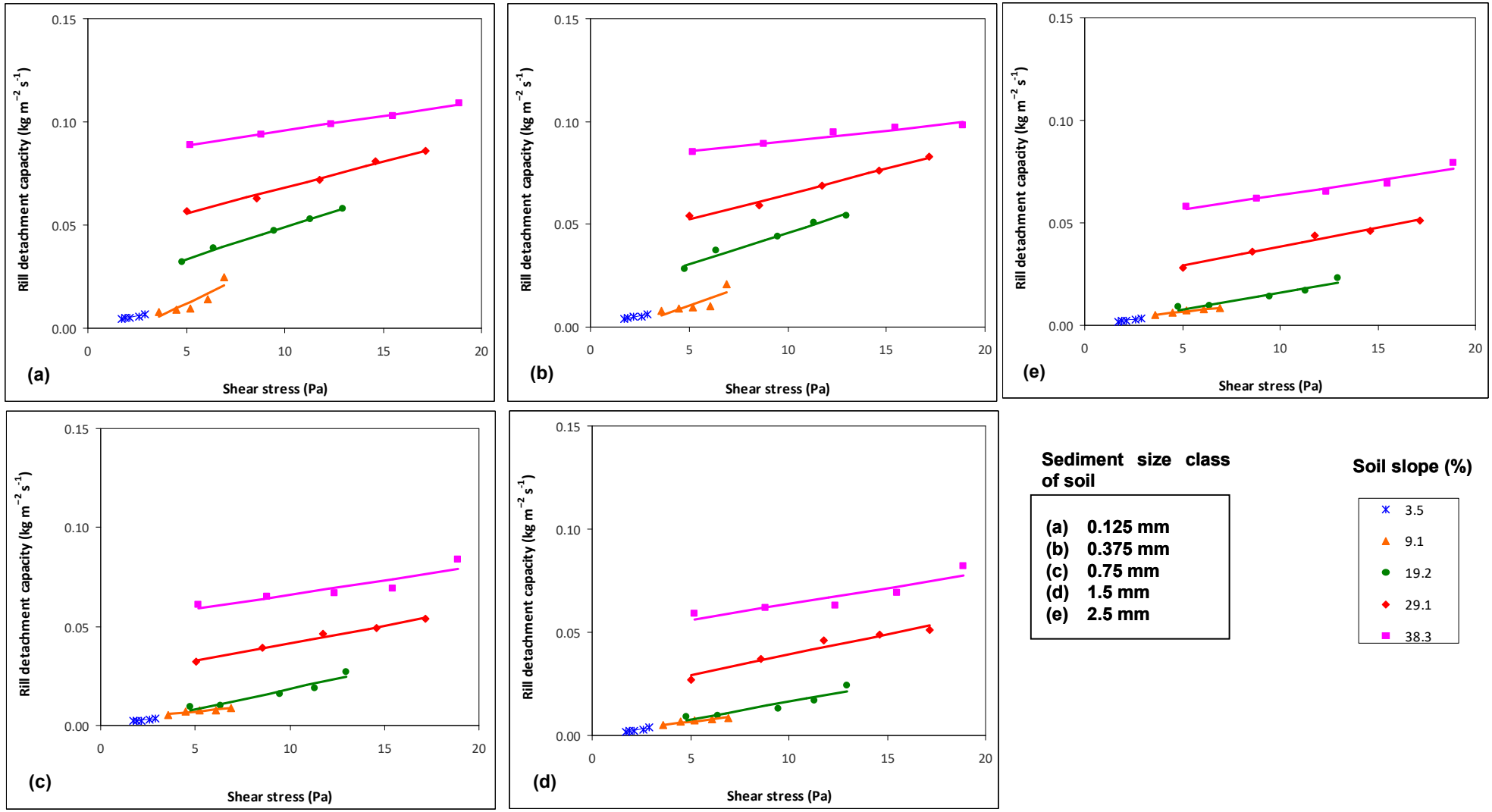
Rill detachment capacity (kg m^{-2} s^{-1})
Shear stress (Pa)
(a)
(b)
(c)
(d)
(e)
0.15
0.10
0.05
0.00
0
5
10
15
20
Sediment size class of soil
(a) 0.125 mm
(b) 0.375 mm
(c) 0.75 mm
(d) 1.5 mm
(e) 2.5 mm
Soil slope (%)
3.5
9.1
19.2
29.1
38.3

309

310 Figure 5 - Linear regressions between the rill detachment capacity and shear stress at different soil slopes and for different sediment size classes of
311 the soil sampled in Saqalaksar Forestland Park (Northern Iran).

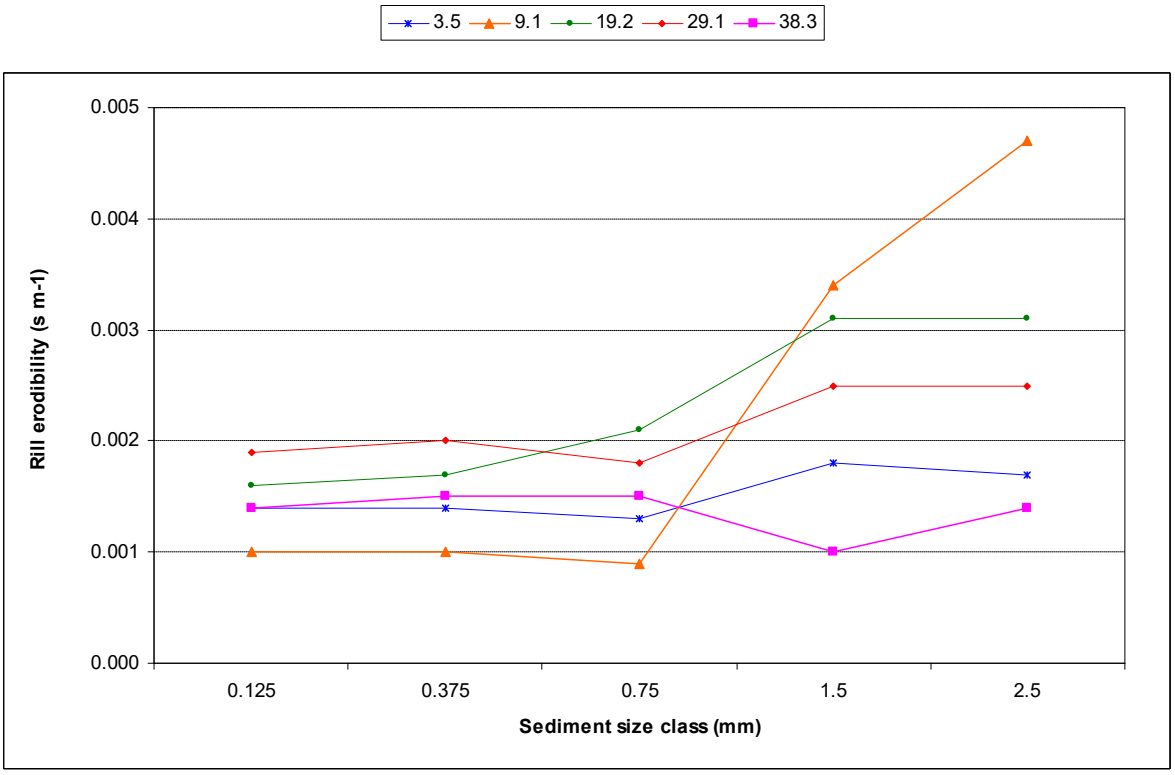

Figure 6 - Variability of rill erodibility for different soil slopes sediment size classes of the soil sampled in Saqalaksar Forestland Park (Northern Iran).

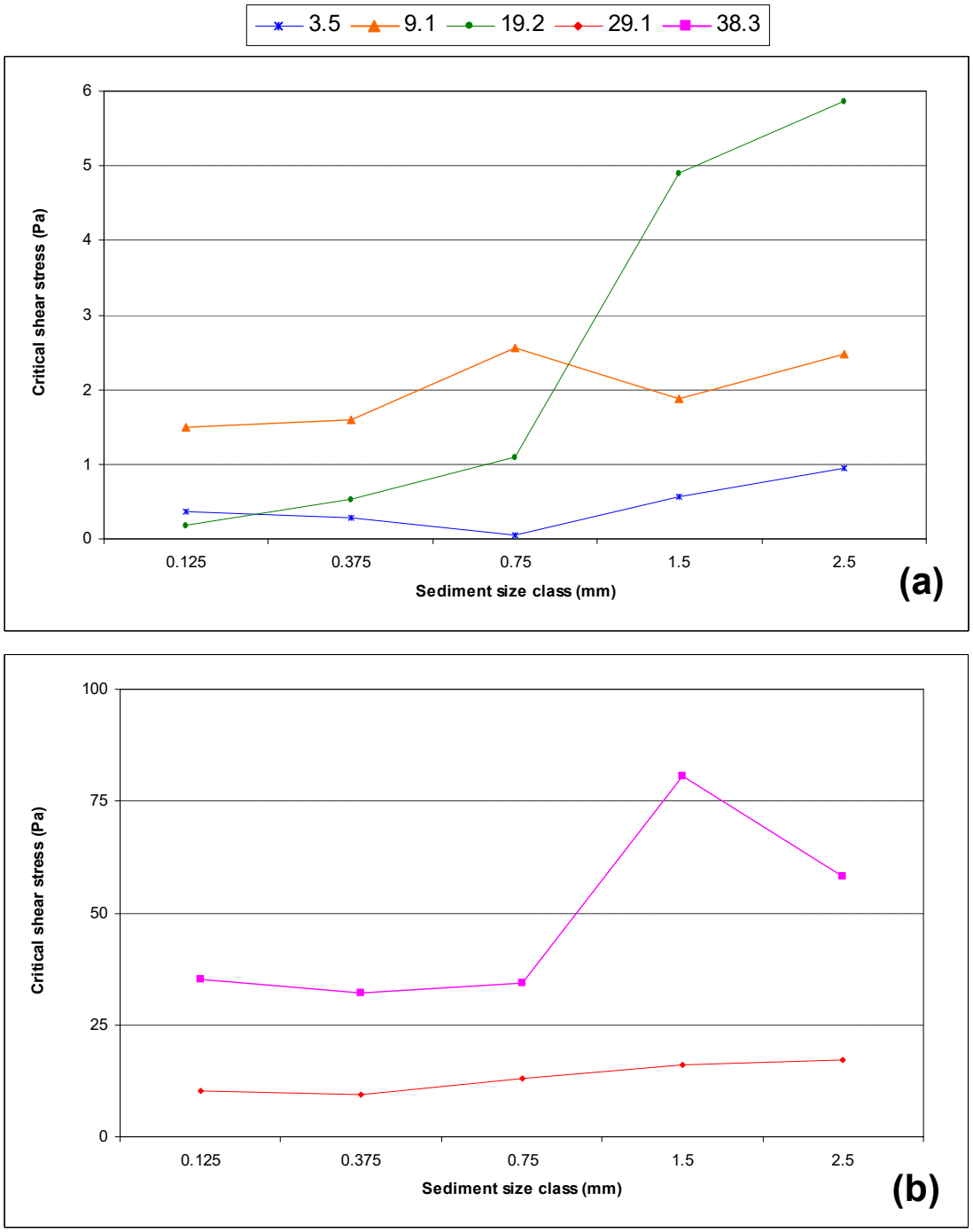

Figure 7 - Variability of critical shear stress for different soil slopes and sediment size classes of the soil sampled in Saqalaksar Forestland Park (Northern Iran).

4. Discussion

The influence of sediment size on soil detachment has been widely investigated, but the contrasting results of the studies have suggested an analysis in hillslopes with variable steepness in reforested areas of Northern Iran. The experimental study at the laboratory

scale has confirmed that rill detachment, which is the dominant erosion agent in slopes with the highest gradients, is different from finer to coarser sediments (Ali et al., 2012; Liu et al., 2019). In more detail, under the same flow rate, the variations in rill detachment capacity among the five sediment size classes under investigation were noticeable, with significantly higher rill detachment capacity for sediments size higher than 1 mm and lower compared to size smaller than 1 mm. This result could be explained by four reasons. First, the flow energy is mainly spent to detach the sediments of higher size, which leads to a lower detachment rate for finer classes. This is in accordance with Liu et al. (2019), who stated that the flow energy consumed to maintain coarser particles in motion for transport is not available to detachment the finer fractions of soil. Second, the coarser sediments are looser compared to finer particles (which include also silty and clayey fractions), and the lack of resisting forces between particles, as indicated by the tensile strength, contributes to increase the detachment rate for medium to coarser sandy particles. Third, the unit surface of the finer particles (that is, the area per unit weight or volume) of soil is higher compared to the fractions of higher size, and, therefore, the drag force act on higher surface of sediment, decreasing shear stress. Therefore, lower shear stress results in lower soil detachment. This is again consistent with the literature, which shows that, in shallow surface flow, the tensile strength and the bursting force of particles can affect the detachment rates (e.g., Nearing et al., 1991). Four, also flow turbulence plays an important role in driving soil detachment. Coarser particles are subject to lower turbulence (e.g., Liu et al., 2019), and this reduction hinders the ability of sediments of higher size to be lifted and flushed downstream by the water flow.

The rill detachment capacity measured in the experimental flume increased with water depth for all sediment classes, and this can be explained by the increasing flow rates. This is in accordance with other works (Nearing et al., 1991; Zhang et al., 2002), who stated that soil detachment rates are a function of flow depth, since particle detachment is more intense with increased flow rate and depth (Zhang et al., 2002). Moreover, the higher the bed slope, the higher is the rill detachment rate for all sediment classes, and therefore also the soil slope plays an important role in driving the rill detachment rate. However, the equations of Table 3 show that the effect of water depth on rill detachment capacity is lower at milder soil gradients compared to steeper soil at all sediment sizes, as shown by the equation slopes (increasing with bed slope). Presumably, higher slopes increases the dragging forces on the soil particles exerted by the overland flow compared to soils with lower slopes, which, in contrast, are less erodible. In other words, rill detachment is generally less

362 sensitive to changes in flow depth than in slope gradient. Our results agree with Zhang et al.
363 (2002), who highlighted the large influence of soil slope on the particle, particularly at the
364 higher gradients, using a similar flume under the same soil slopes; moreover, the effect of
365 flow depth on soil detachment rate is also dependent on slope gradient (Zhang et al., 2002).
366 The combined effect of water depth and bed slope on soil detachment capacity is
367 analytically expressed by the shear stress, which is proportional to the bed slope multiplied
368 by the hydraulic radius (which is in turn dependent on the flow depth). About the modelling
369 approach of this study, several hydraulic parameters of overland flow are descriptors of
370 water properties and this can be used to predict soil detachment capacity (Nearing et al.,
371 1991). Several studies have tried to develop mathematical relations between hydraulic
372 parameters and rill detachment capacity by overland flow (Zhang et al., 2003; Xiao et al.,
373 2017; Li et al., 2019; Wu et al., 2019), also in forest areas (Parhizkar et al., 2020c; 2021b).
374 This study has confirmed that, also in planted forestland, the stream power and its unit
375 value are better descriptors of rill detachment capacity compared to the other flow variables
376 tested in the flume experiments (mean velocity and energy) and ω shows the best prediction
377 capacity of rill detachment at all the investigated sediment size classes, and particularly for
378 the coarser size (mean diameter higher than 1.5 mm). This is close accordance with the
379 collection of power regression models developed in the previous study by Parhizkar et al.
380 (2021a), which was carried out in the same forestland, but without exploring the model
381 accuracy for sediments of different size. The very good prediction capacity of power
382 equations based on unit stream power derives from the fact that this hydraulic parameter
383 considers the flow velocity and soil slope at the same time, and both the latter variables
384 affect soil detachability due to the overland flow (Parhizkar et al., 2020a). In addition,
385 Wang et al. (2018) showed that the unit stream power as input of power functions is a
386 reliable prediction of soil detachment capacity, while Zhang et al. (2002) proposed other
387 hydraulic parameters to model soil detachment process.
388 Soil resistance to rill erosion can be estimated from the rill erodibility (K_r) and critical shear
389 stress (τ_c) (Nearing et al., 1989). Wang et al. (2016) and Parhizkar et al. (2020a; 2021a)
390 have highlighted the linkage of these parameters to the rill detachment capacity. Compared
391 to previous literature, this study has focused the impacts of the sediment size classes on
392 these two parameters in forestlands. In this context, the linear regressions between D_c and τ
393 must be individually developed for each sediment size class rather than for the whole soil
394 samples, and this specific modelling approach is consistent with the variability of rill
395 detachment with sediment size that has been previously analyzed. More equations with

regression coefficients varying with slope and sediment size simulate better reflects the different effects that the drivers of rill detachment process previously identified (i.e., flow energy, sediment size, unit surface of particles, and flow turbulence) play on soil erodibility due to concentrated flow. In any case, the high to extremely high coefficients of determination of the developed regression models show the high accuracy of these equations in predicting the rill erodibility and critical shear stress. This result is consistent with the conclusions of Zhang et al. (2008) and Parhizkar et al. (2020a), who reported the high accuracy in linear equations regressing D_c and τ. Considering that K_r and τ_c are two of the most important parameters reflecting soil resistance to rill erosion (Nearing et al., 1989), the values of these variables proposed in this study can help modellers for accurate predictions of rill erosion in process-based models that are very sensitive to reliable input (Geng et al., 2017; Wang et al., 2016; Knapen et al., 2008). This study has shown that also K_r and τ_c are highly variable with sediment size and slope of soil, both increasing from finer to coarser classes and from milder to steeper profiles. The increase in these parameters in sediment classes with size larger than 1 mm confirms the higher detachability of coarser soil fractions and, of course, high-slope soils, and again shows less resisting force between soil particles in these classes.

5. Conclusions

This study has evaluated the influence of sediment size on rill detachment capacity of a reforested soil using an experimental flume at variable flow rates and bed slopes. Rill detachment capacity was significantly higher for sediments size over 1 mm compared to the other soil fractions. This result has been explained by the combined effects of flow energy and turbulence as well as of particle size and unit surface. Moreover, rill detachment capacity was more influenced by bed slope compared to water depth. Therefore, the first working hypothesis of the current study (significant variations of rill detachment capacity with sediment size) can be confirmed.

Power regression models were developed to assess the rill detachment capacity by hydraulic parameters for each sediment size class. The unit stream power as input parameter of power equations is the best predictor of rill detachment at all the investigated particle size classes. Linear regression models between rill detachment capacity and shear stress were very accurate in predicting both rill erodibility and critical shear stress, provided that these models are developed and calibrated separately for different sediment size classes

of soil. Therefore, also the second hypothesis of the current study (need to consider the rill detachment variability with particle size) can be confirmed. The modelling approach of the study has again confirmed that soil particles with size higher than 1 mm have a lower resistance to rill erosion compared to the finer fractions.

Overall, the study is a contribution to a better understanding of a key process of soil erosion, such as particle detachment, on which particle size plays a high influence. Furthermore, the results of the modelling activity propose values of the rill erodibility and critical shear stress to be used by land planners in process-based erosion models.

Acknowledgements

The authors thank the Faculty of Agricultural Sciences, University of Guilan for their support and experimental assistance.

References

Abrahams, A.D., Parsons, A.J., Luk, S.H., 1985. Field measurement of the velocity of overland flow using dye tracing. Earth Surf. Process. Landf. 11: 653–657.

Ali, M., Sterk, G., Seeger, M., Stroosnijder, L., 2012. Effect of flow discharge and median grain size on mean flow velocity under overland flow. J. Hydrol. 452–453, 150–160.

Bagnold, R.A., 1966. An approach to the sediment transport problem for general physics. In U.S. Geological Survey Professional Paper 422-I; U.S. Government Printing Office: Washington, DC, USA.

Borrelli, P., Alewell, C., Alvarez, P., Anache, J.A.A., Baartman, J., Ballabio, C., ... Panagos, P. 2021. Soil erosion modelling: A global review and statistical analysis. Science of The Total Environment, 146494.

Bezak, N., Mikoš, M., Borrelli, P., Alewell, C., Alvarez, P., … Panos Panagos, Soil erosion modelling: A bibliometric analysis. Environmental Research, 2021, 111087.

Cerdà, A., Novara, A., Dlapa, P., López-Vicente, M., Úbeda, X., Popović, Z., Mekonnen, M., Terol, E., Janizadeh, S., Mbarki, S., Saldanha Vogelmann, E., Hazrati, S., Sannigrahi, S., Parhizkar, M., Giménez-Morera, A., 2021. Rainfall and water yield in Macizo del Caroig, Eastern Iberian Peninsula. Event runoff at plot scale during a rare flash flood at the

Barranco de Benacancil. Cuadernos de Investigación Geográfica 47, http://doi.org/10.18172/cig.4833.

De Baets, S., Poesen, J., Gyssels, G., Knapen, A., 2006. Effects of grass roots on the erodibility of topsoils during concentrated flow. Geomorphology. 76, 54–67.

Foster, G.R., 1982. Modeling the erosion process. In Hydrologic Modeling of Small Watersheds; Haan, C.T., Ed.; ASAE: St. Joseph, MI, USA, pp. 296–380.

Geng, R., Zhang, G.H., Ma, Q.H., Wang, L.J., 2017. Soil resistance to runoff on steep croplands in Eastern China. Catena. 152: 18–28.

Hairsine, P.B., and Rose, C.W. 1992 Modeling water erosion due to overland flow using physical principles, II. Rill flow. Water Resour. Res. 28, 237–243.

Jiang, F., He, K., Huang, M., Zhang, L., Lin, G., Zhan, Z., Li, H., Lin, I., Håkansson, J., Ge, H., Huang, Y., 2020. Impacts of near soil surface factors on soil detachment process in benggang alluvial fans. Journal of Hydrology. 590: 125274.

Knapen, A., Poesen, J., Govers, G., De Baets, S., 2008. The effect of conservation tillage on runoff erosivity and soil erodibility during concentrated flow. Hydrol. Process. 22: 1497–1508.

Kottek, M., Grieser, J., Beck, C., Rudolf, B., Rubel, F., 2006. World Map of the Koppen-Geiger climate classification updated. Meteorol. Z. 15: 259–263.

Li, M., Hai, X., Hong, H., Shao, Y., Peng, D., Xu, W., Yang, Y., Zheng, Y., Xia, Z., 2019. Modelling soil detachment by overland flow for the soil in the Tibet Plateau of China. Sci. Rep. 9: 8063, doi:10.1038/s41598-019-44586-5.

Li, Z.W., Zhang, G.H., Geng, R., Wang, H., Zhang, X.C., 2015. Land use impacts on soil detachment capacity by overland flow in the Loess Plateau, China. Catena. 124: 9–17.

Liu, J., Zhou, Z., Zhang, X.J., 2019. Impacts of sediment load and size on rill detachment under low flow discharges. Journal of Hydrology. 570: 719–725.

Merten, G.H., Nearing, M.A., Borges, A.L.O., 2001. Effect of sediment load on soil detachment and deposition in rills. Soil Sci. Soc. Am. J. 65 (3): 861–868.

Morgan, R.P., Quinton, J.N., Smith, R.E., Govers, G., Poesen, J.W.A., Auerswald, K.; Chisci, G., Torri, D., Styczen, M.E. 1998. The European soil erosion model (EUROSEM): A dynamic approach for predicting sediment transport from fields and small catchments. Earth Surf. Process. Landf. 23, 527–544.

Moriasi, D.N., Arnold, J.G., Van Liew, M.W., Bingner, R.L., Harmel, R.D., Veith, T.L., 2007. Model evaluation guidelines for systematic quantification of accuracy in watershed simulations. Trans. ASABE. 50: 885–900.

498 Nash, J.E., Sutcliffe, J.V., 1970. River flow forecasting through conceptual models part I-a
499 discussion of principles. J. Hydrol. 10: 282–290.
500 Nearing, M.A., Bradford, J.M., Parker, S.C., 1991. Soil detachment by shallow flow at low
501 slopes. Soil Sci. Soc. Am. J. 55: 339–344.
502 Nearing, M.A., Foster, G.R., Lane, L.J., Finkner, S.C., 1989. A process-based soil erosion
503 model for USDA-Water Erosion Prediction Project technology. Trans. ASAE. 32: 1587–
504 1593.
505 Nearing, M.A., Simanton, J.R., Norton, L.D., Bulygin, S.J., Stone, J., 1999. Soil erosion by
506 surface water flow on a stony, semiarid hillslope. Earth Surf. Process. Landf. 24: 677–686.
507 Nearing, M.A., Foster, G.R., Lane, L.J., Finkner, S.C., 1989. A process-based soil erosion
508 model for USDA-Water Erosion Prediction Project technology. Trans. ASAE. 32: 1587–
509 1593.
510 Parhizkar, M., Shabanpour, M., Khaledian, M., Asadi, H., 2021a. The evaluation of soil
511 detachment capacity induced by vegetal species based on the comparison between natural
512 and planted forests. Journal of Hydrology. 595: 126041.
513 Parhizkar, M., Shabanpour, M., Khaledian, M., Cerdà, A., Rose, C.W., Asadi, H., Lucas-
514 Borja, M.E., Zema, D.A., 2020a. Assessing and Modeling Soil Detachment Capacity by
515 Overland Flow in Forest and Woodland of Northern Iran. Forests. 11(1): 65.
516 Parhizkar, M., Shabanpour, M., Lucas-Borja, M.E., Zema, D.A., Li, S., Tanaka, N., Cerdà,
517 A., 2020b. Effects of length and application rate of rice straw mulch on surface runoff and
518 soil loss under laboratory simulated rainfall. International Journal of Sediment Research, In
519 press.
520 Parhizkar, M., Shabanpour, M., Miralles, I., Cerdà, A., Tanaka, N., Asadi, H., Lucas-Borja,
521 M.E., Zema, D.A., 2021b. Evaluating the effects of forest tree species on rill detachment
522 capacity in a semi-arid environment. Ecological Engineering. 161: 106158.
523 Parhizkar, M., Shabanpour, M., Miralles, I., Zema, D.A., Lucas-Borja, M.E., 2021c. Effects
524 of plant species on soil quality in natural and planted areas of a forest park in northern
525 Iran. Science of the Total Environment. 778: 146310.
526 Parhizkar, M., Shabanpour, M., Zema, D.A., Lucas-Borja, M.E., 2020c. Rill Erosion and
527 Soil Quality in Forest and Deforested Ecosystems with Different Morphological
528 Characteristics. Resources 9 (11): 129.
529 Parhizkar, M., Shabanpour, M., Lucas-Borja, M.E., Zema, D.A. 2021d. Hydromulch roots
530 reduce rill detachment capacity by overland flow in deforested hillslopes. Journal of
531 Hydrology.

Pollen, N., 2007. Temporal and spatial variability in root reinforcement of stream banks: accounting for soil shear strength and moisture. Catena. 69, 197–205.

Rodrigo-Comino, J., Keesstra, S., Cerdà, A., 2018. Soil erosion as an environmental concern in vineyards: the case study of Celler del Roure, Eastern Spain, by means of rainfall simulation experiments. Beverages. 4(2): 31.

Shabanpour, M., Daneshyar, M., Parhizkar, M., Lucas-Borja, M.E., Zema, D.A., 2020. Influence of crops on soil properties in agricultural lands of northern Iran. Science of The Total Environment. 711: 134694.

Shen, N., Wang, Z., Zhang, Q., Chen, H., Wu, B., 2019. Modelling soil detachment capacity by rill flow with hydraulic variables on a simulated steep loessial hillslope. Hydrology Research. 50 (1): 85–98.

Singh, J., Knapp, H.V., Demissie, M., 2004. Hydrologic Modeling of the Iroquois River Watershed Using HSPF and SWAT. ISWS CR 2004–2008. Champaign, Ill.: Illinois State Water Survey. Available online: http://www.sws.uiuc.edu/pubdoc/CR/ISWSCR2004-08.pdf (accessed on 20 February 2021).

Van Liew, M.W., Garbrecht, J., 2003. Hydrologic simulation of the Little Washita River experimental watershed using SWAT. J. Am. Water Resour. Assoc. 39: 413–426.

Vannoppen, W., Vanmaercke, M., De Baets, S., Poesen, J., 2015. A review of the mechanical effects of plant roots on concentrated flow erosion rates. Earth Sci. Rev. 150, 666–678.

Vannoppen, W., De Baets, S., Keeble, J., Dong, Y., Poesen, J., 2017. How do root and soil characteristics affect the erosion-reducing potential of plant species? Ecol. Eng. 109, 186–195.

Wang, B., Zhang, G.H., Shi, Y.Y., Zhang, X.C., 2014. Soil detachment by overland flow under different vegetation restoration models in the Loess Plateau of China. Catena. 116: 51–59.

Wang, B., Zhang, G.H., Yang, Y.F., Li, P.P., Liu, J.X., 2018. The effects of varied soil properties induced by natural grassland succession on the process of soil detachment. Catena. 166: 192–199.

Wang, D.D., Wang, Z.L., Shen, N., Chen, H., 2016. Modeling soil detachment capacity by rill flow using hydraulic parameters. J. Hydrol. 535: 473–479.

Wang, D.D., Wang, Z.L., Shen, N., Chen, H., Modeling soil detachment capacity by rill flow using hydraulic parameters. J. Hydrol. 2016: 535, 473–479.

565 Wu, B., Wang, Z.L., Zhang, Q.W., Shen, N., Liu, J., 2019. Response of soil detachment
566 rate by raindrop-affected sediment-laden sheet flow to sediment load and hydraulic
567 parameters within a detachment limited sheet erosion system on steep slopes on Loess
568 Plateau, China. Soil & Tillage Research. 185: 9–16.
569 Xiao, H., Liu, G., Liu, P.L., Zheng, F.L., Zhang, J.Q., Hu, F.N., 2017. Response of soil
570 detachment rate to the hydraulic parameters of concentrated flow on steep loessial slopes on
571 the loess plateau of China. Hydrol. Process. 31: 2613–2621.
572 Yang, C.T., 1972. Unit stream power and sediment transport. J. Hydrol. Div. ASCE. 98:
573 1805–1826.
574 Zhang, G.H., Liu, B.Y., Liu, G.B., He, X.W., Nearing, M.A., 2003. Detachment of
575 undisturbed soil by shallow flow. Soil Sci. Soc. Am. J. 67: 713–719.
576 Zhang, G.H., Liu, B.Y., Nearing, M.A., Huang, C.H., Zhang, K.L., 2002. Soil detachment
577 by shallow flow. Trans. ASAE. 45: 351–357.
578 Zhang, G.H., Liu, G.B., Tang, K.M., Zhang, X.C., 2008. Flow detachment of soils under
579 different land uses in the Loess Plateau of China. Trans. ASABE. 51: 883–890.